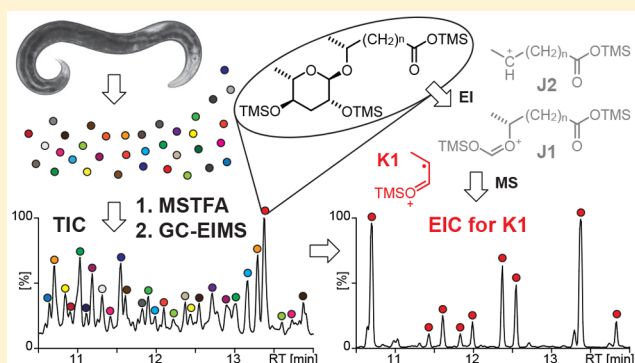


Ascaroside Profiling of *Caenorhabditis elegans* Using Gas Chromatography–Electron Ionization Mass SpectrometryStephan H. von Reuss,^{*,†,‡,§} Franziska Dolke,[†] and Chuanfu Dong^{†,§}[†]Department of Bioorganic Chemistry, Max Planck Institute for Chemical Ecology, D-07745 Jena, Germany

Supporting Information

ABSTRACT: Nematodes such as the model organism *Caenorhabditis elegans* produce various homologous series of L-ascarylose-derived glycolipids called ascarosides, which include several highly potent signals in intra and interspecies communication as well as cross-kingdom interactions. Given their low concentrations and large number of structurally similar components, mass spectrometric screens based on high-performance liquid chromatography–electrospray ionization–tandem mass spectrometry (HPLC-ESI-MS/MS) are commonly employed for ascaroside detection and quantification. Here, we describe a complementary gas chromatography–electron ionization mass spectrometry (GC-EIMS) screen that utilizes an ascarylose-derived K1-fragment ion signal at m/z 130.1 $[C_6H_{14}OSi]^+$ to highlight known as well as yet unidentified ascaroside components in TMS-derivatized crude nematode exometabolome extracts. GC-EIMS-based ascaroside profiling of wild-type and mutant *C. elegans* facilitates the analysis of all basic ascarosides using the same ionization technique while providing excellent resolution for the complete homologous series with side chains ranging from 3 to 33 carbons. Combined screening for m/z 130.1 along with side chain-specific J1 $[M - 173]^+$ and J2 $[M - 291]^+$ fragment ions, as well as additional characteristic marker ions from α -cleavage, enables convenient structure assignment of ca. 200 components from wild-type and peroxisomal β -oxidation mutants including ($\omega - 1$)-linked acyl, enoyl, β -hydroxyacyl, and 2-ketoalkyl ascarosides along with their (ω)-linked or α -methyl isomers and ethanolamide derivatives, as well as 2-hydroxyalkyl ascarosides. Given the widespread availability of GC-MS and its increasing popularity in metabolomics, this method will promote the identification of ascarosides in *C. elegans* and other nematodes.



The model organism *Caenorhabditis elegans* releases several homologous glycolipid series based on the 3,6-dideoxy-L-arabino-hexopyranose L-ascarylose (Figure 1), which control its

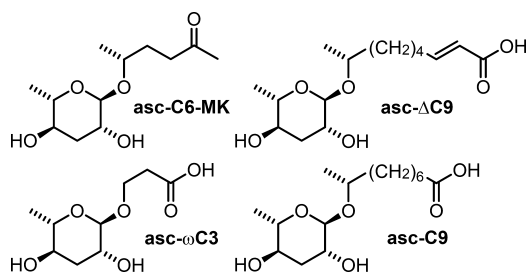


Figure 1. Basic ascarosides from *Caenorhabditis elegans*.

developmental plasticity and behavior.^{1–4} For example, a synergistic blend including asc-C6-MK (ascr#2),⁵ asc- Δ C9 (ascr#3),⁵ and asc- ω C3 (ascr#5)⁶ functions in dauer formation and competition between different genotypes.⁷ Asc- Δ C9 (ascr#3) also acts as a hermaphrodite repellent, whereas the predominantly male-produced asc-C9 (ascr#10) acts as a potent hermaphrodite attractant,⁸ demonstrating that small

changes in the ascaroside side chains can have a severe impact on biological activities. In addition, the basic ascaroside skeletons also serve as scaffolds for species-specific attachment of additional units originating from primary metabolic pathways to furnish complex modular assemblies.^{9,10} Ascarosides have been identified in multiple nematode species and shown to modulate diverse biological functions,^{11–17} demonstrating that ascaroside signaling is conserved in nematodes. Furthermore, ascarosides are also implicated in cross kingdom interactions, such as modulation of plant defenses,¹⁶ coordination of host beetle metamorphosis with nematode dispersal,¹⁷ and trap formation in nematophagous fungi,¹⁸ suggesting that ascarosides represent key regulators in nematode ecology.

Detection and quantification of homologous ascaroside series has commonly been accomplished using RP-C18-HPLC-MS and more than 150 components have previously been described from wild-type and mutant *C. elegans*.¹⁹ For highest sensitivity, targeted analysis with selected reaction monitoring (SRM) and

Received: July 18, 2017

Accepted: September 3, 2017

Published: September 3, 2017

electrospray ionization in positive mode (ESI(+))^{20–22} or negative mode (ESI(-))^{23–25} has been employed. Furthermore, an ESI(-)-MS/MS precursor ion screen has been developed that utilizes a characteristic ascarylose-derived fragment ion at m/z 73.1 $[C_3H_5O_2]^-$ to detect known as well as yet unidentified ascarioside components.¹⁹ MS/MS precursor ion screening has proven extremely powerful in various studies^{11–17,25–27} but ultimately requires a triple quadrupole mass spectrometer that is not universally available in many research laboratories. Furthermore, ESI(-)-MS/MS screening fails to ionize nonacidic ascariosides such as the potent *C. elegans* dauer inducing asc-C6-MK (ascr#2)⁵ or its dihydro-derivative asc-C6-OH (ascr#6).²⁸ These compounds ionize well using ESI(+), which, however, results in complex spectra due to in source fragmentation (ISCID) and the formation of diverse adducts such as $[M + H]^+$, $[M + Li]^+$, $[M + NH_4]^+$, $[M + Na]^+$, and $[M + K]^+$. Some of these adducts do not represent efficient precursors for MS/MS analysis, which so far has precluded the development of a general ascarioside-selective screen based on ESI(+), apart from a targeted screen for indole ascariosides that employs an ISCID-derived fragment ion as characteristic marker.¹⁰

Furthermore, there currently exists no protocol for the chromatographic separation of the complete homologous ascarioside series. Standard HPLC methods using RP-C18 columns result in poor peak shape and low sensitivity for the highly polar short chain components such as asc- ω C3 (ascr#5).^{6,19} Furthermore, upon gradient elution with acetonitrile as mobile phase long chain ascariosides with side chains exceeding 22 carbons are not eluted.¹⁹ However, biosynthetic studies using comparative metabolomics with *C. elegans* peroxisomal β -oxidation mutants revealed that ascarioside biogenesis involves chain shortening of very long chain precursors that feature side chains with up to 33 carbons.^{19,29} Similar very long chain ascariosides that carry 2-hydroxyalkyl side chains with 29, 31, and 33 carbons have been described from the *C. elegans* wild-type exometabolome^{28,30} as well as the eggs of *Ascaris suum*.³¹ For HPLC analysis of these lipophilic components, nonpolar solvent systems such as acetonitrile/isopropanol with C18-columns^{28,29} or C8-columns eluted with methanol³⁰ have been employed, which are unsuitable to resolve the large diversity of short chain components.

Considering these challenges, we have explored the suitability of GC-MS for ascarioside profiling. Gas chromatography–electron ionization mass spectrometry (GC-EIMS) analysis of TMS-derivatized carbohydrates and glycosides constitutes a powerful analytical method developed more than 50 years ago,³² which provides excellent separation along with a wealth of structural information from electron ionization (EI)-induced fragmentation.^{33–37} A direct probe EIMS analysis of very long chain 2-hydroxyalkyl ascariosides,³⁸ as well as GC–flame ionization detector (FID) analysis of their trimethylsilyl (TMS) derivatives,³⁹ has previously been described.

Here we present the development of a highly selective ascarioside screen using GC-EIMS analysis of TMS-derivatized crude nematode exometabolome extracts that facilitates the detection of diverse ascariosides carrying side chains from 3 to 33 carbons and provides structural information for the various aglycones. Given the widespread availability of GC-MS, we anticipate that this method will be of great value for nematode research in diverse disciplines. Furthermore, as GC-EIMS analysis of TMS derivatives is widely applied in metabolomics⁴⁰ and becomes increasingly popular in *C. elegans* research,^{41–46}

this study also serves to identify a large number of MS-features commonly encountered in nematode exometabolomes.

■ EXPERIMENTAL SECTION

Chemicals and Reagents. Authentic reference standards of 15 ascariosides were synthesized as previously described (Figure S1). The short chain asc-C3 and asc-C4 (ascr#11) and homologous mixtures dominated by the long chain asc-C18 (ascr#32) or asc- ω C20 (oscr#34), as well as asc-C11-EA (easc#18) from *Heterorhabditis bacteriophora*¹⁴ were prepared as described in the Supporting Information. Rhannolipids from *Pseudomonas aeruginosa* were from AGAE technologies. *N*-Methyl-*N*-(trimethylsilyl)trifluoroacetamide (MSTFA) was from Macherey-Nagel.

Nematode Strains and General Culture Methods. *Caenorhabditis elegans* wild-type strain N2 (Bristol) as well as peroxisomal β -oxidation mutants *acox-1(ok2257)*I strain VC178S, *maoc-1(hj13)*II strain VS18, *dhs-28(hj8)*X strain VS8, and *daf-22(ok693)*II strain RB859 were cultivated at 23 °C on solidified nematode growth medium (NGM agar) seeded with *E. coli* OP50.

Preparation of Nematode Exometabolome Extracts. Liquid cultures were established in 100 mL of S-medium at 23 °C and 150 rpm using mixed stage nematodes from three 10 cm plates collected in M9 buffer as inoculums. Concentrated *E. coli* OP50 bacteria pellet from an overnight culture in Lysogeny Broth (LB) medium at 37 °C and 170 rpm was provided as food from day 1 until 6 after which the cultures were harvested. Culture supernatant representing the exometabolome was collected by centrifugation (5 min at 5000 g), filtered, frozen at –80 °C, lyophilized, and extracted with 2 × 50 mL methanol for 12 h each. The combined extract was filtered, concentrated to dryness at 40 °C under reduced pressure, and reconstituted in methanol for HPLC-MS and GC-MS analysis.

Fractionation of Nematode Exometabolomes. Crude nematode exometabolome extract from 100 mL cultures was fractionated using solid phase extraction (SPE) on 500 mg reverse phase C18 cartridges (Chrompack, Macherey Nagel) using a stepwise 10% increase of methanol concentrations in water as eluent. Inorganic salts eluted in the flow-through and initial aqueous fraction, whereas short, medium, long, and very long chain ascariosides were eluted in subsequent fractions of increasing methanol content. Fractions of 3 mL each were concentrated to dryness at 30 °C under reduced pressure using a centrifugal vacuum concentrator (Eppendorf).

Preparation of Trimethylsilyl (TMS) Derivatives for GC-EIMS Analysis. Aliquots of authentic ascarioside standard solutions (10 μ L of 100 μ g/mL solution), crude nematode exometabolome extracts, or their fractions were concentrated to dryness. The residues were treated with 10 μ L of *N*-methyl-*N*-(trimethylsilyl)trifluoroacetamide (MSTFA) at 60 °C for 40 min, diluted with 10 μ L DCM, and 1 μ L of the solution analyzed by GC-EIMS.

Preparation of Methyl Ester Derivatives for GC-EIMS Analysis. Aliquots of ascarioside standard solutions (1 μ L of 100 μ g/mL solution) were concentrated to dryness. The residues were dissolved in 200 μ L of a 1:1 mixture of methanol and toluene and treated with 20 μ L 2.0 M trimethylsilyldiazomethane solution in diethyl ether. After stirring at RT for 1 h the excess reagent was quenched by addition of 20 μ L of acetic acid and the reaction mixtures concentrated to dryness. The residues were subsequently treated with MSTFA as described

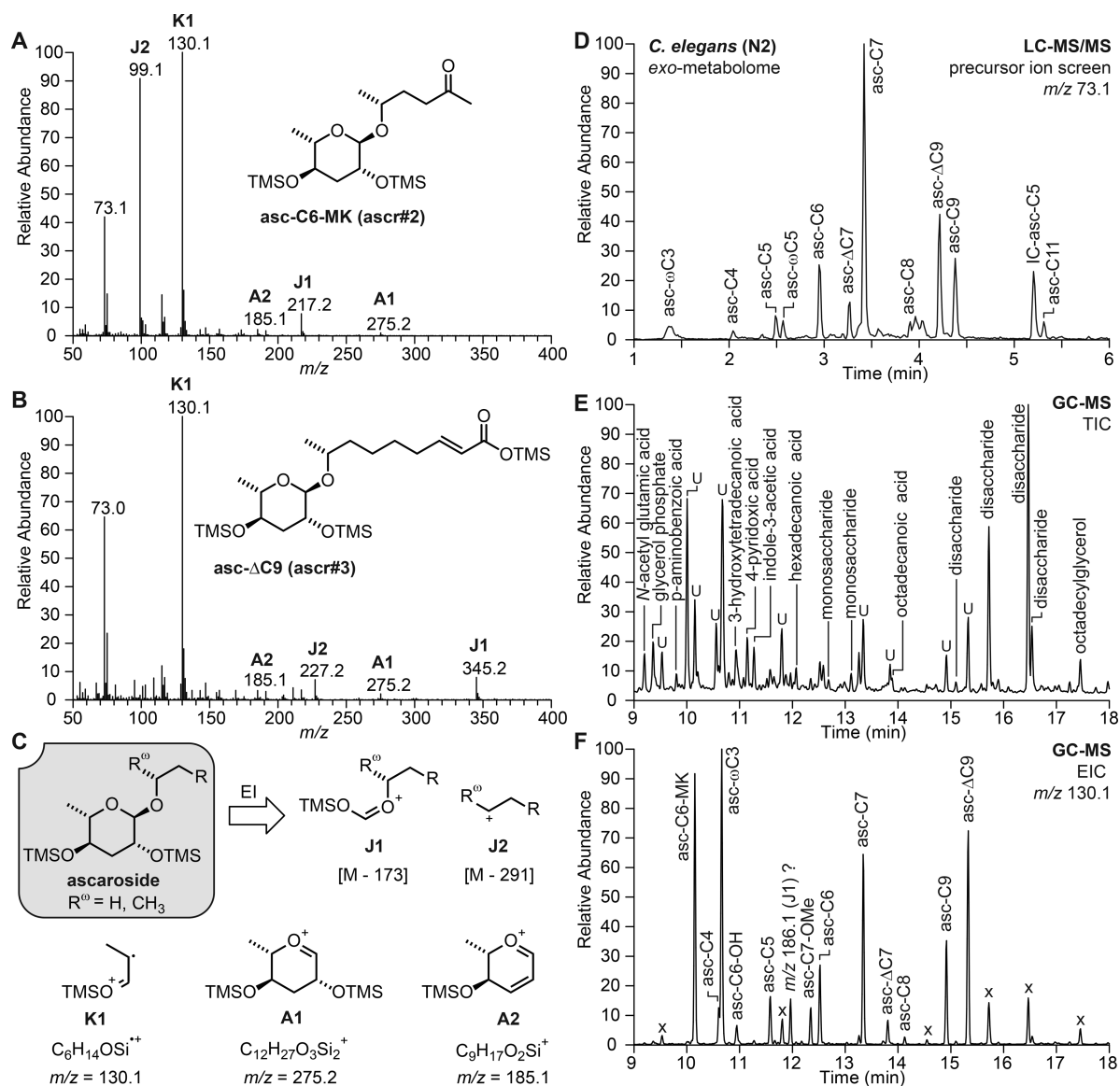


Figure 2. Development of a GC-EIMS based ascaroside screen. EIMS spectra of TMS-derivatized ascaroside standards of (A) asc-C6-MK (ascr#2) or (B) asc- Δ C9 (ascr#3); for other ascaroside standards, see Figure S1. (C) Characteristic EIMS fragments observed for TMS-derivatized ascarosides according to standard nomenclature.^{33,35} (D) Total ion chromatogram (TIC) from HPLC-MS/MS precursor ion screening of the *C. elegans* wild-type exometabolome extract. (E) TIC from GC-EIMS analysis of the TMS-derivatized *C. elegans* wild-type exometabolome extract with structure assignments derived from comparison with the NIST14 library, U = unknown. (F) Extracted ion chromatogram (EIC) for the K1-fragment at m/z 130.1 $[C_6H_{14}OSi]^+$ shows almost exclusively signals corresponding to ascarosides, X = false positive, ? = unidentified ascaroside component.

above to afford the TMS derivatives of the methyl esters for GC-EIMS analysis.

Gas Chromatography–Electron Ionization–Mass Spectrometry (GC-EIMS). The separation of volatile TMS derivatives and acquisition of their 70 eV electron ionization mass spectra was performed using a Trace GC 2000 series (Thermo Scientific) coupled to a ThermoQuest Trace MS (Finnigan). Chromatographic separations were achieved using a Zebron ZB-5 Guardian column (15 m, 0.25 mm ID, 0.25 μ m film thickness, with 10 m guardian end) with helium as the carrier gas at a flow rate of 1 mL/min. A temperature program starting at 130 $^{\circ}$ C for 5 min, followed by a linear gradient of +10 $^{\circ}$ C/min to 350 $^{\circ}$ C was applied. A total volume of 1 μ L was injected using a 10:1 split ratio and an injector temperature of 250 $^{\circ}$ C. Mass spectra were acquired from m/z 35–650 amu.

For the determination of Kovats retention indices, a C_7 – C_{40} alkane standard mixture was employed.

Liquid Chromatography–Electrospray Ionization–High-Resolution Tandem Mass Spectrometry (HPLC-ESI-HR-MS/MS). HPLC-ESI-HR-MS/MS analysis of ascaroside standard solutions, crude nematode exometabolome extracts, and their fractions was performed using a Dionex UltiMate 3000 HPLC instrument coupled to a Bruker Maxis high resolution qTOF mass spectrometer equipped with an electrospray ionization (ESI) unit operated in positive or negative mode. Chromatographic separations were achieved using an Agilent ZORBAX Eclipse XDB-C18 column (250 \times 3 mm, 5 μ m particle diameter) with a flow rate of 400 μ L/min and gradient elution starting at 3% acetonitrile in 0.5% aqueous acetic acid for 5 min followed by a linear increase to 100% acetonitrile with 0.5% acetic acid within 35 min. For highly

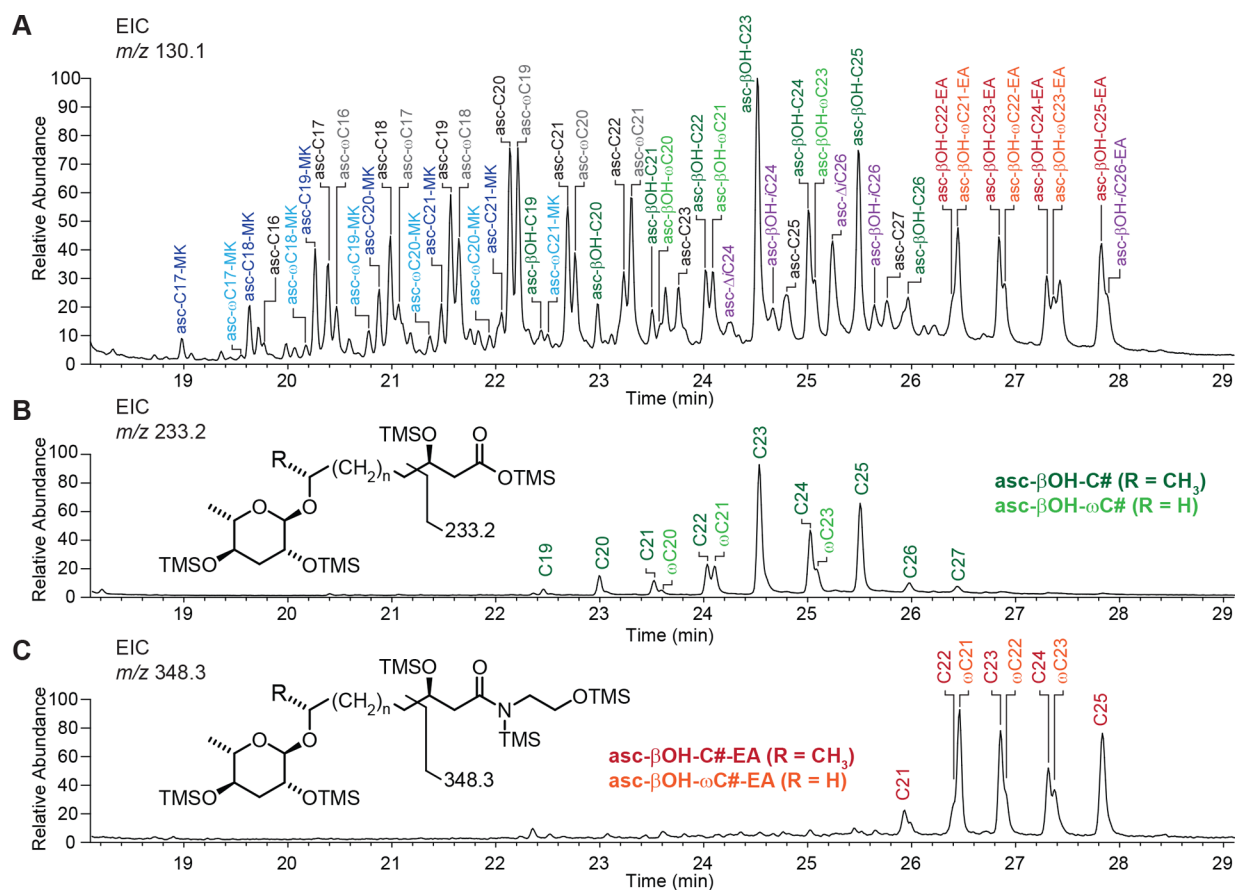


Figure 3. GC-EIMS analysis of TMS-derivatized long and very long chain ascarosides from a *C. elegans* *daf-22* mutant exometabolome fraction. (A) EIC for the K1-fragment at m/z 130.1 $[C_6H_{14}OSi]^+$ shows a large diversity of homologous long chain ascarosides. (B) EIC for m/z 233.1 $[C_9H_{21}O_3Si_2]^+$ from α -cleavage specifically highlights β -hydroxyacyl ascarosides. (C) EIC for m/z 348.2 $[C_{14}H_{34}NO_3Si_3]^+$ from α -cleavage specifically highlights β -hydroxyacyl ascaroside ethanolamides.

lipophilic, very long chain ascarosides, gradient elution starting at 100% acetonitrile with 0.5% aqueous acetic acid for 5 min followed by a linear increase to 75% isopropanol in 25% acetonitrile with 0.5% acetic acid within 35 min was employed.

Liquid Chromatography–Electrospray Ionization–Precursor Ion Screening. HPLC-MS/MS precursor ion screening for m/z 73.1 was performed using an Agilent 1260 HPLC instrument (Agilent Technologies) coupled to an API5000 Triple Quadrupole LC/MS/MS mass spectrometer (AB Sciex, Darmstadt) equipped with an electrospray ionization (ESI) unit operated in negative mode. A CID energy of -34 was applied. Chromatographic separations were achieved using an Agilent ZORBAX Eclipse XDB-C18 column (50×4.6 mm, $1.8 \mu\text{m}$ particle diameter) (Agilent Technologies) with a flow rate of 1.1 mL/min and gradient elution starting at 5% acetonitrile in 0.05% aqueous formic acid followed by a linear increase to 95% acetonitrile with 0.05% formic acid within 10 min.

RESULTS

GC-EIMS Analysis of TMS-Derivatized Ascarosides.

Aiming to develop a GC-MS method for the analysis of nematode-derived ascarosides, a collection of authentic reference standards were converted into their trimethylsilyl (TMS) derivatives using *N*-methyl-*N*-(trimethylsilyl)-trifluoroacetamide (MSTFA) and subsequently analyzed by GC-MS. Most of the 20 ascarosides tested formed volatile TMS

derivatives suitable for GC-MS analysis (Figure S1), including asc-C6-MK (ascr#2) and asc- Δ C9 (ascr#3), the dominating dauer inducing components of the *C. elegans* population density cue (Figure 2A–B).⁵ Simple derivatives could also be analyzed such as the dihydroxylated dhas#18, a male-produced female attractant in *Panagrellus redivivus* (Figure S2),¹² or the ethanolamide derivative asc-C11-EA (easc#18), a population density cue that triggers development of infective juveniles in entomopathogenic *Heterorhabditis bacteriophora* (Figure S3).¹⁴ However, more complex derivatives such as the indole ascarosides (icas#2,¹⁰ icas#3⁹) could not be analyzed by GC-MS.

A comparative analysis of the 70 eV electron ionization mass spectra revealed several common fragment ion signals characteristic for the ascarylose unit along with a variety of side chain-specific signals. Most importantly a highly conserved base peak for an ascarylose-derived K1-fragment at m/z 130.1 $[C_6H_{14}OSi]^+$ was observed, along with minor oxonium ion signals at m/z 275.1 $[C_{12}H_{27}O_3Si_2]^+$ (A1) and m/z 185.1 $[C_9H_{17}O_2Si]^+$ (A2) (Figure 2A–C), which, taken together represent suitable markers for 3,6-dideoxy-*arabino*-hexopyranosides like the nematode ascarosides. In contrast, 6-deoxy-*manno*-pyranosides such as the rhamnolipids from *Pseudomonas aeruginosa* exhibit only an insignificant signal at m/z 130.1 but instead show a dominating H1a-fragment at m/z 204.1 $[C_8H_{20}O_2Si_2]^+$,³⁶ which is generally considered as characteristic marker for glycopyranosides^{33–37} but almost absent in the

mass spectra of TMS-derivatized ascarosides (Figure S4). While no signal for the molecular ion or the corresponding $[M - \text{CH}_3]^+$ fragment ion was observed, EI-induced fragmentation involves the formation of a rearranged oxonium ion representing a J1-fragment at $[M - 173]^+$ along with a carbocation at $[M - 291]^+$ (J2) from loss of the ascarylose unit (Figure 2C). Structure assignment of these side chain-specific fragments was subsequently confirmed by comparative analyses of the mass spectra of TMS-derivatized homologous ascarosides and their methyl esters (Figure S5). Taken together, these side chain-specific signals are highly characteristic and allow the molecular weight of the aglycone to be deduced.

A Selective GC-EIMS Screen for Nematode Ascarosides. Having established that GC-MS represents a powerful method for the analysis of TMS-derivatized ascarosides, we evaluated its applicability for ascaroside screening of nematode exometabolomes. GC-EIMS analysis of the MSTFA-treated crude exometabolome extract of wild-type *C. elegans* (N2), previously shown by HPLC-MS/MS precursor ion screening to contain a complex mixture of ascarosides (Figure 2D),¹⁹ revealed a diversity of primary and secondary metabolites, some of which could be tentatively assigned by comparison with the NIST 14 mass spectral library (Figure 2E). An inspection of the extracted ion chromatogram (EIC) for m/z 130.1 $[\text{C}_6\text{H}_{14}\text{OSi}]^+$, the common K1-fragment observed as the base peak signal for all ascaroside standards tested, shows almost exclusively signals corresponding to ascaroside components (Figure 2F), thus facilitating their detection even in unfractionated nematode exometabolome extracts. Most importantly, the GC-MS screen enables the analysis of all basic ascarosides including the main dauer inducing components asc-C6-MK (ascr#2) and asc- Δ C9 (ascr#3) using the same ionization method (Figure 2A–B,F). Furthermore, GC provides excellent resolution and peak shape even for highly polar short chain components such as asc- ω C3 (ascr#5) (Figure 2F), which is only poorly retained by HPLC (Figure 2D). However, in contrast to HPLC-MS/MS precursor ion screening the GC-MS screen fails to detect any of the more complex ascaroside derivatives such as the indole ascarosides (e.g., IC-asc-C5, aka icas#9), which play important functions in species-specific signaling.¹⁰ While GC-MS is consequently limited to the most basic ascaroside components it does facilitate the detection of various simple derivatives, some of which are not readily detectable by ESI(-)-MS techniques such as the methyl ester of ascr#1 (asc-C7-OMe), which might represent an artifact of sample processing, or a yet unidentified nitrogen containing derivative with a J2-fragment at m/z 186.1 (Figure 2F). False positives in GC-MS-based ascaroside profiling (labeled “X”) are predominantly due to $[M + 1]$ signals of unidentified minor components that exhibit intensive signals at m/z 129.1 or minor fragment ion signals from highly dominating components (e.g., carbohydrates), both of which can be easily determined by the inspection of the corresponding mass spectra.

GC-MS Ascaroside Screening Facilitates the Analysis of Very Long Chain Ascarosides from *C. elegans* Mutant Metabolomes. To evaluate the scope of the GC-MS screen, the exometabolome of *C. elegans* mutants carrying defects in peroxisomal β -oxidation was analyzed. Acyl-CoA oxidase *aco-1*, enoyl-CoA hydratase *maoc-1*, 3-hydroxyacyl-CoA dehydrogenase *dhs-28*, and 3-ketoacyl-S-CoA thiolase *daf-22* mutants accumulate a diversity of long and very long chain ascarosides, the biosynthetic intermediates of the short chain components

prominent in wild-type worms.^{19,29} To reduce the amount of nonvolatile components and increase the concentration of specific analytes, a fractionation step using RP-C18 was employed, which also reduces the number of overlapping peaks in highly complex mixtures such as the *daf-22* metabolome (Figure 3) and facilitates the identification of even very minor components that might otherwise be missed upon screening of crude metabolome extracts (Figure S6). Analyses of exometabolome fractions from peroxisomal β -oxidation mutants demonstrate that GC-EIMS screening facilitates the detection of ($\omega - 1$)- and (ω)-linked ascarosides carrying side chains with up to 33 carbons including acyl (asc-C#), enoyl (asc- Δ C#), β -hydroxyacyl (asc- β OH-C#), and 2-oxoalkyl (asc-C#-MK) moieties along with their α -methyl isomers (asc-*i*C#) and ethanolamide derivatives (asc-C#-EA), as well as (2*R*)-hydroxyalkyl (asc-C#-OH) moieties (Tables S1–20). In addition to the ascaroside-specific K1-fragment at m/z 130.1 $[\text{C}_6\text{H}_{14}\text{OSi}]^+$ aglycone-specific J1- and J2-fragment ions were identified for each compound, which, along with the Kovats retention indices, enable unambiguous compound identification. Plotting of Kovats retention indices versus carbon number of the aglycones affords the anticipated linear correlations for the various homologous series (Figure S7), which supports the assignment of ascaroside structures for which no reference standards are yet available. A compilation of compound specific qualifier ions along with their Kovats retention indices for about 200 ascarosides is provided in Tables S1–20. Furthermore, structure assignments were independently confirmed by HPLC-HR-MS(/MS) analysis (Tables S21–38). In conclusion, the analysis of *C. elegans* wild-type and mutant metabolomes demonstrates that GC-EIMS represents a powerful tool for the characterization of the entire homologous series of ascarosides ranging from short to very long chain components and thus is particularly well-suited for ascaroside profiling in biosynthetic studies and characterization of *C. elegans* mutants with defects in peroxisomal β -oxidation.

EI-Induced Fragmentation Facilitates the Structure Assignment of Ascaroside Aglycones. Considering that electron ionization represents a hard ionization technique that results in significant fragmentation, we further analyzed the mass spectra of ascarosides aiming to identify characteristic fragments that could aid in structure assignment of the aglycone or be used to screen for homologous ascaroside series. We first focused on β -hydroxyacyl ascarosides, which represent biosynthetic intermediates in the peroxisomal β -oxidation pathway.¹⁹ An analysis of the mass spectrum of a TMS-derivatized asc- β OH-C13 (bhas#22) standard revealed a diagnostic fragment ion signal at m/z 233.1 $[\text{C}_9\text{H}_{21}\text{O}_3\text{Si}_2]^+$ due to α -cleavage (Figure S1c). Combined screening for both m/z 130.1 and m/z 233.1 thus facilitates convenient assignment of ($\omega - 1$)- and (ω)-linked homologous β -hydroxyacyl ascarosides as shown for a *daf-22* mutant exometabolome fraction (Figure 3B). Furthermore, combined screening for m/z 130.1 and m/z 247.1 $[\text{C}_{10}\text{H}_{23}\text{O}_3\text{Si}_2]^+$ even facilitates the detection of α -methyl-branched β -hydroxy-*iso*-acyl ascarosides, such as asc- β OH-*i*C24 and asc- β OH-*i*C26 (Figures 3A and S8), whose acyl and enoyl derivatives have previously been described from the *daf-22* metabolome (Figures S9–10).²⁹

In the same way, combined screening for m/z 130.1 and m/z 348.2 $[\text{C}_{14}\text{H}_{34}\text{NO}_3\text{Si}_3]^+$ enables the assignment of ($\omega - 1$) and (ω)-linked homologous series of β -hydroxyacyl ascaroside ethanolamides, asc- β OH-C#-EAs (Figure 3C), whereas m/z

130.1 along with m/z 362.2 $[\text{C}_{15}\text{H}_{36}\text{NO}_3\text{Si}_3]^+$ reveals an α -methyl-branched β -hydroxy-*iso*-acyl ascaroside ethanolamide, asc- β OH-*i*C26-EA (Figure S11), structurally related to the previously described enoyl ethanolamide derivatives from the *daf-22* metabolome (Figure S12).²⁹

Furthermore, we found that EIMS spectra of TMS-derivatized ascarosides also depend on the linkage of the aglycone via the terminal (ω)-carbon or the penultimate ($\omega - 1$)-carbon. Both (ω)- and ($\omega - 1$)-linked ascarosides afford the characteristic oxonium ion signals at $[\text{M} - 173]^+$ (J1), but the signal intensity for the side chain-derived carbocation at $[\text{M} - 291]^+$ (J2) is considerably more pronounced for ($\omega - 1$)-ascarosides (Figure 4), reflecting the fact that the formation of

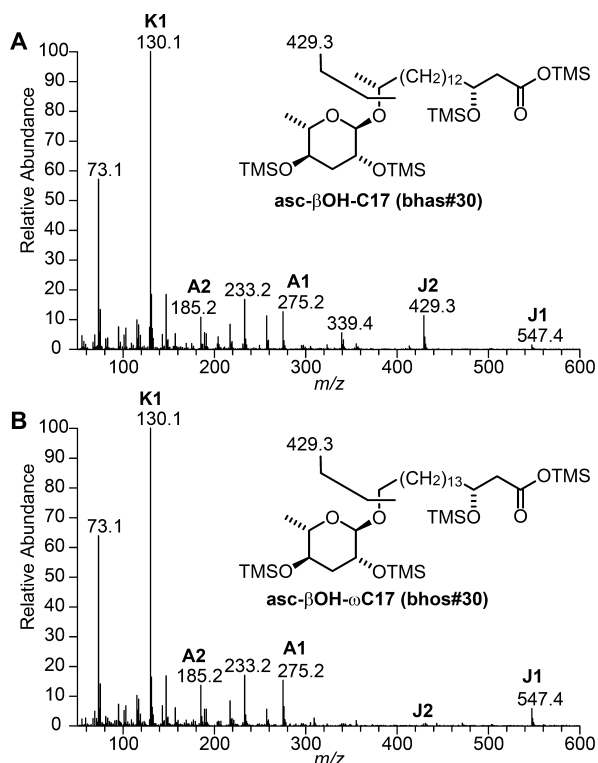


Figure 4. Side chain-specific fragments facilitate discrimination of ($\omega - 1$) and (ω)-linked ascarosides. MS spectrum of TMS-derivatized asc- β OH-C17 (bhas#30) (A) shows a characteristic J1-fragment at m/z 547.4 along with a prominent J2-fragment at m/z 429.3 from loss of the ascrylose unit, which is attenuated in the later eluting (ω)-linked isomer asc- β OH- ω C17 (bhos#30) (B).

the corresponding carbocation from (ω)-linked ascarosides is highly disfavored (Figure S13). Consequently, in the presence of both (ω)- and ($\omega - 1$)-ascarosides, the analysis of Kovats retention indices along with EIMS spectra facilitates their structure assignment. Taken together, these results demonstrate how characteristic fragment ions could aid in structure assignment of the aglycones or be employed to screen for homologous ascaroside series.

Similarly, the inspection of the mass spectrum of a TMS-derivatized asc-C6-OH (ascr#6.1) standard as a representative for 2-hydroxyalkyl ascarosides revealed a characteristic fragment ion signal at m/z 117.1 $[\text{C}_5\text{H}_{13}\text{OSi}]^+$ originating from α -cleavage, as well as aglycone-specific carbocations at m/z 173.1 $[\text{C}_9\text{H}_{21}\text{OSi}]^+$ (J2) and m/z 83.1 $[\text{C}_6\text{H}_{11}]^+$ (J2 - TMSOH) (Figure 5A). GC-EIMS screening of *C. elegans* exometabolome fractions for components exhibiting both m/z 130.1 and m/z

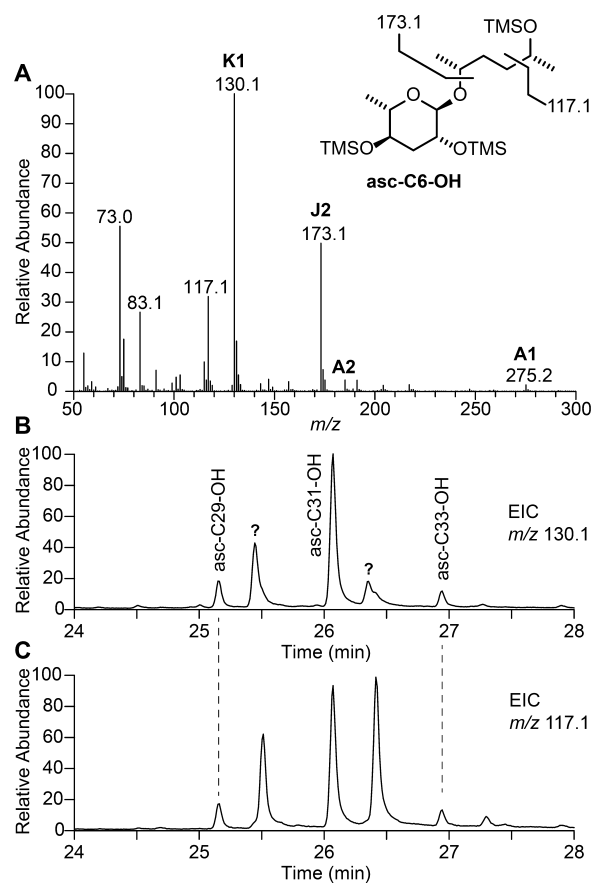


Figure 5. Side chain-specific fragments facilitate screening for 2-hydroxyalkyl ascarosides. (A) GC-EIMS spectrum of TMS-derivatized asc-C6-OH reveals a characteristic fragment at m/z 117.1 $[\text{C}_5\text{H}_{13}\text{OSi}]^+$ from α -cleavage. Extracted ion chromatograms for m/z 130.1 (B) and m/z 117.1 (C) of a highly lipophilic TMS-derivatized *C. elegans* exometabolome fraction show three very long chain 2-hydroxyalkyl ascarosides.

117.1 revealed three very long chain 2-hydroxyalkyl ascarosides dominated by asc-C31-OH (Figures 5B–C) that were previously detected by LC-MS.^{28,30} Comparative analysis of *C. elegans* wild-type and mutant exometabolomes further demonstrated that the biosynthesis of these highly lipophilic 2-hydroxyalkyl ascarosides is largely independent of peroxisomal β -oxidation by *acox-1*, *maoc-1*, *dhs-28*, and *daf-22* (Figure S14).

CONCLUSIONS

GC-EIMS-based ascaroside profiling represents a powerful technique that utilizes a highly characteristic K1-fragment ion at m/z 130.1 $[\text{C}_6\text{H}_{14}\text{OSi}]^+$ to promote the detection of a large diversity of known as well as yet unidentified basic ascarosides even in unfractionated nematode exometabolome extracts. The method combines the excellent resolution achieved by gas chromatography (facilitating the resolution of various homologous ascaroside series with side chains ranging from 3 to 33 carbons and differentiation of ($\omega - 1$)- and (ω)-linked as well as α -methyl branched isomers) with the wealth of structural information derived from EI-induced fragmentations (facilitating the assignment of aglycone structures based on side chain-specific J1 and J2-fragment ions and additional marker ions from α -cleavage). Given the widespread availability of GC-MS,

this methodology will promote the characterization of ascarosides in *C. elegans* and other nematodes.

■ ASSOCIATED CONTENT

Supporting Information

The Supporting Information is available free of charge on the ACS Publications website at DOI: 10.1021/acs.analchem.7b02803.

Additional figures and tables as indicated in the text, synthetic procedures, and NMR spectra for ascaroside standards (PDF)

■ AUTHOR INFORMATION

Corresponding Author

* E-mail: stephan.vonreuss@unine.ch. Phone: +41-32-7182510. Fax: +41-32-7182511.

ORCID

Stephan H. von Reuss: 0000-0003-4325-5495

Present Addresses

[‡]S.H.v.R.: Laboratory of Bioanalytical Chemistry, Institute of Chemistry, University of Neuchâtel, Avenue de Bellevaux 51, CH-2000 Neuchâtel, Switzerland.

[§]C.D.: Department of Integrative Evolutionary Biology, Max Planck Institute for Developmental Biology, Spemannstraße 35, D-72076 Tübingen, Germany.

Notes

The authors declare no competing financial interest.

■ ACKNOWLEDGMENTS

Financial support by the Max Planck Society (MPG) and the Jena School for Microbial Communication (JSMC) is gratefully acknowledged. Some ascaroside standards were kindly provided by Prof. Frank C. Schroeder (BTI, Cornell University, Ithaca, US). We also thank Dr. Michael Reichelt (Department for Biochemistry, MPICE, Jena) for acquisition of the MS/MS precursor ion screen and Kerstin Ploss for technical assistance. Nematode strains were provided by the *Caenorhabditis* Genetics Center, which is funded by NIH Office of Research Infrastructure Programs (P40 OD010440).

■ REFERENCES

- (1) von Reuss, S. H.; Schroeder, F. C. *Nat. Prod. Rep.* **2015**, *32*, 994–1006.
- (2) Schroeder, F. C. *Chem. Biol.* **2015**, *22*, 7–16.
- (3) Butcher, R. A. *Nat. Chem. Biol.* **2017**, *13*, 577–586.
- (4) Butcher, R. A. *Nat. Prod. Rep.* **2017**, *34*, 472–477.
- (5) Butcher, R. A.; Fujita, M.; Schroeder, F. C.; Clardy, J. *Nat. Chem. Biol.* **2007**, *3*, 420–422.
- (6) Butcher, R. A.; Ragains, J. R.; Kim, E.; Clardy, J. *Proc. Natl. Acad. Sci. U. S. A.* **2008**, *105*, 14288–14292.
- (7) Diaz, S. A.; Brunet, V.; Lloyd-Jones, G. C.; Spinner, W.; Wharam, B.; Viney, M. *BMC Evol. Biol.* **2014**, *14*, 46.
- (8) Izrayelit, Y.; Srinivasan, J.; Campbell, S. L.; Jo, Y.; von Reuss, S. H.; Genoff, M. C.; Sternberg, P. W.; Schroeder, F. C. *ACS Chem. Biol.* **2012**, *7*, 1321–1325.
- (9) Srinivasan, J.; von Reuss, S. H.; Bose, N.; Zaslaver, A.; Mahanti, P.; Ho, M.; O'Doherty, O.; Edison, A. S.; Sternberg, P. W.; Schroeder, F. C. *PLoS Biol.* **2012**, *10*, e1001237.
- (10) Dong, C. F.; Dolke, F.; von Reuss, S. H. *Org. Biomol. Chem.* **2016**, *14*, 7217–7225.
- (11) Choe, A.; von Reuss, S. H.; Kogan, D.; Gasser, R. B.; Platzer, E. G.; Schroeder, F. C.; Sternberg, P. W. *Curr. Biol.* **2012**, *22*, 772–780.
- (12) Choe, A.; Chuman, T.; von Reuss, S. H.; Dossey, A. T.; Yim, J.; Ajredini, R.; Kolawa, A. A.; Kaplan, F.; Alborn, H. T.; Teal, P. E.; Schroeder, F. C.; Sternberg, P. W.; Edison, A. S. *Proc. Natl. Acad. Sci. U. S. A.* **2012**, *109*, 20949–20954.
- (13) Bose, N.; Ogawa, A.; von Reuss, S. H.; Yim, J. J.; Sommer, R. J.; Schroeder, F. C. *Angew. Chem., Int. Ed.* **2012**, *51*, 12438–12443.
- (14) Noguez, J. H.; Conner, E. S.; Zhou, Y.; Ciche, T. A.; Ragains, J. R.; Butcher, R. A. *ACS Chem. Biol.* **2012**, *7*, 961–966.
- (15) Chaudhuri, J.; Bose, N.; Adams, S.; Zuco, G.; Tandonnet, S.; Naia, T.; Kache, V.; Parihar, M.; von Reuss, S. H.; Schroeder, F. C.; Pires-daSilva, A. *Sci. Rep.* **2015**, *5*, 17676.
- (16) Manosalva, P.; Manohar, M.; von Reuss, S. H.; Chen, S.; Koch, A.; Kaplan, F.; Choe, A.; Micikas, R. J.; Wang, X.; Kogel, K.-H.; Sternberg, P. W.; Williamson, V. M.; Schroeder, F. C.; Klessig, D. F. *Nat. Commun.* **2015**, *6*, 7795.
- (17) Zhao, L.; Zhang, X.; Wei, Y.; Zhou, J.; Zhang, W.; Qin, P.; Chinta, S.; Kong, X.; Liu, Y.; Yu, H.; Hu, S.; Zou, Z.; Butcher, R. A.; Sun, J. *Nat. Commun.* **2016**, *7*, 12341.
- (18) Hsueh, Y. P.; Mahanti, P.; Schroeder, F. C.; Sternberg, P. W. *Curr. Biol.* **2013**, *23*, 83–86.
- (19) von Reuss, S. H.; Bose, N.; Srinivasan, J.; Yim, J. J.; Judkins, J. C.; Sternberg, P. W.; Schroeder, F. C. *J. Am. Chem. Soc.* **2012**, *134*, 1817–1824.
- (20) Joo, H. J.; Yim, Y.-H.; Jeong, P.-Y.; Jin, Y.-X.; Lee, J.-E.; Kim, H.; Jeong, S.-K.; Chitwood, D. J.; Paik, Y.-K. *Biochem. J.* **2009**, *422*, 61–71.
- (21) Joo, H.-J.; Kim, K.-Y.; Yim, Y.-H.; Jin, Y.-X.; Kim, H.; Kim, M.-Y.; Paik, Y.-K. *J. Biol. Chem.* **2010**, *285*, 29319–29325.
- (22) Kim, K. Y.; Joo, H.-J.; Kwon, H.-W.; Kim, H.; Hancock, W. S.; Paik, Y.-K. *Anal. Chem.* **2013**, *85*, 2681–2688.
- (23) Noh, K.; Park, J. H.; Park, J. H.; Kim, M.; Jung, M.; Ha, H.; Kwon, K.; Lee, H. J.; Kang, W. J. *Pharm. Biomed. Anal.* **2011**, *56*, 114–117.
- (24) Noh, K.; Park, J. H.; Kim, M.; Jung, M.; Lee, H. J.; Kwon, K.; Kang, W.; Ha, H. *Biomed. Chromatogr.* **2012**, *26*, 152–155.
- (25) Artyukhin, A. B.; Yim, J. J.; Srinivasan, J.; Izrayelit, Y.; Bose, N.; von Reuss, S. H.; Jo, Y.; Jordan, J. M.; Baugh, L. R.; Cheong, M.; Sternberg, P. W.; Avery, L.; Schroeder, F. C. *J. Biol. Chem.* **2013**, *288*, 18778–18783.
- (26) Zhang, X.; Feng, L.; Chinta, S.; Singh, P.; Wang, Y.; Nunnery, J. K.; Butcher, R. A. *Proc. Natl. Acad. Sci. U. S. A.* **2015**, *112*, 3955–3960.
- (27) Zhang, X.; Noguez, J. H.; Zhou, Y.; Butcher, R. A. Analysis of Ascarosides from *Caenorhabditis elegans* Using Mass Spectrometry and NMR Spectroscopy. In *Pheromone Signaling: Methods and Protocols, Methods in Molecular Biology*, Vol. 1068; Kazushige, T., Ed.; Springer Science + Business Media, LLC, 2013; pp 71–92.
- (28) Pungaliya, C.; Srinivasan, J.; Fox, B. W.; Malik, R. U.; Ludewig, A. H.; Sternberg, P. W.; Schroeder, F. C. *Proc. Natl. Acad. Sci. U. S. A.* **2009**, *106*, 7708–7713.
- (29) Izrayelit, Y.; Robinette, S. L.; Bose, N.; von Reuss, S.; Edison, A. S.; Schroeder, F. C. *ACS Chem. Biol.* **2013**, *8*, 314–319.
- (30) Zagoriy, V.; Matyash, V.; Kurzchalia, T. *Chem. Biodiversity* **2010**, *7*, 2016–2022.
- (31) Bartley, J. P.; Bennett, E. A.; Darben, P. A. *J. Nat. Prod.* **1996**, *59*, 921–926.
- (32) Sweeley, C. C.; Bentley, R.; Makita, M.; Wells, W. W. *J. Am. Chem. Soc.* **1963**, *85*, 2497–2507.
- (33) Kotchetov, N. K.; Chizhov, O. S. *Adv. Carb. Chem.* **1966**, *21*, 39–93.
- (34) DeJongh, D. C.; Radford, T.; Hribar, J. D.; Hanessian, S.; Bieber, M.; Dawson, G.; Sweeley, C. C. *J. Am. Chem. Soc.* **1969**, *91*, 1728–1740.
- (35) Petržika, M.; Linow, F. *Eur. J. Mass Spectrom. Biochem., Med. Environ. Res.* **1982**, *2*, 53–61.
- (36) De Bettignies-Dutz, A.; Reznicek, G.; Kopp, B.; Jurenitsch, J. *J. Chromatogr.* **1991**, *547*, 299–306.
- (37) Doco, T.; O'Neill, M. A.; Pellerin, P. *Carbohydr. Polym.* **2001**, *46*, 249–259.
- (38) Tarr, G. E.; Schnoes, H. K. *Arch. Biochem. Biophys.* **1973**, *158*, 288–296.

- (39) Tarr, G. E.; Fairbairn, D. *Lipids* **1973**, *8*, 7–16.
- (40) Lai, Z.; Fiehn, O. *Mass Spectrom. Rev.* **2016**, DOI: 10.1002/mas.21518.
- (41) Geier, F. M.; Want, E. J.; Leroi, A. M.; Bundy, J. B. *Anal. Chem.* **2011**, *83*, 3730–3736.
- (42) Butler, J. A.; Mishur, R. J.; Bokov, A. F.; Hakala, K. W.; Weintraub, S. T.; Rea, S. L. *PLoS One* **2012**, *7*, e46140.
- (43) Castro, C.; Krumsiek, J.; Lehrbach, N. J.; Murfitt, S. A.; Miska, E. A.; Griffin, J. L. *Mol. BioSyst.* **2013**, *9*, 1632–1642.
- (44) Jaeger, C.; Tellstrom, V.; Zurek, G.; Konig, S.; Eimer, S.; Kammerer, B. *Metabolomics* **2014**, *10*, 859–876.
- (45) Van Assche, R.; Temmerman, L.; Dias, D. A.; Boughton, B.; Boonen, K.; Braeckman, B. P.; Schoofs, L.; Roessner, U. *Metabolomics* **2015**, *11*, 477–486.
- (46) Yun, E. J.; Lee, S. H.; Kim, S.; Kim, S. H.; Kim, K. H. *Process Biochem.* **2017**, *53*, 36–43.